$LaCo_2B_2$: A Co-Based Layered Superconductor with a $ThCr_2Si_2$-Type Structure

Hiroshi Mizoguchi,[1] Toshiaki Kuroda,[2] Toshio Kamiya,[2] and Hideo Hosono[1,2,*]

[1]*Frontier Research Center, Tokyo Institute of Technology, 4259 Nagatsuta, Midori-ku, Yokohama 226-8503, Japan*

[2]*Materials and Structures Laboratory, Tokyo Institute of Technology, 4259 Nagatsuta, Midori-ku, Yokohama 226-8503, Japan*

(Received 6 February 2011; published 8 June 2011)

$LaCo_2B_2$ with a $ThCr_2Si_2$-type (so-called "122") structure composed of alternately stacked La and CoB layers exhibits metallic electrical conductivity and Pauli paramagnetic behavior down to 2 K. Bulk superconductivity with a T_c of ~4 K emerges upon substituting with dopant elements, i.e., isovalent substitution to form $(La_{1-x}Y_x)Co_2B_2$, or aliovalent substitution to form $La(Co_{1-x}Fe_x)_2B_2$. According to the density functional theory calculations, highly covalent bonding between Co 3*d* dominating the Fermi level and *B* 2*p* levels deeper than the Fermi level removes magnetic ordering from Co 3*d* electrons even in the undoped samples. This is a first Co-based superconductor among the 122-type family.

DOI: 10.1103/PhysRevLett.106.237001 PACS numbers: 74.70.Xa, 71.20.Ps

Since the discovery of high temperature superconductivity in F-doped LaFeAsO, iron-based layered pnictides including AFe_2As_2 (A = Sr, Ba) and FeSe have attracted much attention because superconductivity with a relatively high superconducting transition (T_c) was observed from their magnetic iron-based parent compounds [1,2]. These pnictides or chalcogenides adopt tetragonal crystal structures that include FeAs layers composed of edge-sharing As tetrahedra with an Fe center within the plane. Doping the parent compound with carriers suppresses the formation of antiferromagnetic (AFM) ordering, resulting in the emergence of superconductivity. Many Ni-based compounds including $LuNi_2B_2C$, $MgCNi_3$, and LaNiPO also exhibit superconductivity [3,4]. These metallic compounds possess Pauli paramagnetic (PM) behavior and exhibit superconducting transitions without the aid of carrier doping. Among these Ni-based compounds, those with a NiB layer, an analog of the FeAs layer in Fe pnictides with respect to structure and the number of valence electrons, have a tendency to exhibit a relatively high T_c (10–15 K) [4]. For the past 25 years it has been known that some late transition metal compounds show superconductivity at low temperature, as evidenced by these compounds composed of Fe, Ni, and Cu. These results suggest that compounds of Co, which is located between Fe and Ni in the periodic table, should exhibit superconducting transitions. Nonetheless, very few reports on superconductive Co-based compounds are available [5,6]; for instance, LaCoPO and LaCoAsO are itinerant ferromagnetic metals but do not exhibit a superconducting transition [7] even though they have the same crystal structure as LaFeAsO.

Here, we report that $LaCo_2B_2$ with a negative Seebeck coefficient exhibits a T_c of ~4 K upon cationic substitution. The parent compound, $LaCo_2B_2$, which was first reported by Niihara *et al*. in 1973 [8], adopts a tetragonal $ThCr_2Si_2$-type (so-called "122") structure, to which more than 700 isostructural compounds including AFe_2As_2 [9–12] belong. It is expected that Co-based materials will be a platform from which to explore new superconductors in the 122-type family, even though their T_c is only moderately high.

Polycrystalline samples of $(La_{1-x}Y_x)Co_2B_2$, $La(Co_{1-x}Fe_x)_2B_2$, and $LaCo_2(B_{1-x}Si_x)_2$ were synthesized by the arc-melting method. Elemental La, Co, B, Y, Fe, and Si were used as starting materials. The arc-melted ingot was annealed at 1273 K in an evacuated silica ampoule when necessary. The chemical compositions of the products were determined using a JXA-8530F electron microprobe analyzer (JEOL). The crystal structures of the synthesized materials were examined by powder x-ray diffraction (XRD) at 300 K using Cu K_α or synchrotron radiation (BL02B2 beam line of SPring-8) with the aid of Rietveld refinements using RIETAN-FP software [13]. The dependence of dc electrical resistivity (ρ) on temperature was measured over 2–300 K by a conventional four-probe method. Magnetization (M) measurements were performed with a vibrating sample magnetometer (Quantum Design).

Spin-polarized density functional theory (DFT) periodic calculations were performed using the Vienna *ab initio* simulation package code [14] with a projector augmented wave method [15,16] and PBE96 generalized gradient approximation (GGA) functional. The GGA + U approximation was applied to the La 4*f* orbitals using the rotational-variant +U method with an effective Coulomb parameter (U_{eff}) of 11 eV [17]. For Co 3*d*, different U_{eff} values varied from 0 to 1.2 eV, whose value is proposed for Fe 3*d* in LaFeAsO [18], were examined. First, quantum-mechanically stable structure was calculated so as to take a self-consistent field energy minimum. Band structure and density of states (DOS) were calculated based on the relaxed structures.

The arc-melted $LaCo_2B_2$ ingots were dark gray in color and possessed a metallic luster. Powder XRD measurements revealed that the crystal structure was of 122-type (space group $I4/mmm$), and the chemical composition

TABLE I. Crystal structure of $LaCo_2B_2$,[a] as determined by Rietveld refinement[b] of a synchrotron XRD data set covering a 2θ range of 3°–70°. The wavelength was resolved to 0.352 90 (1) Å against a CeO_2 standard. Data for the crystal structure obtained from DFT calculations are also shown.

	a (nm)	c (nm)	z(boron)	B(La)(Å^2)	B(Co) (Å^2)	B(boron) (Å^2)
Observed (300 K)	0.361 082(9)	1.020 52(2)	0.3324(5)	0.24(1)	0.27(1)	1.2(1)
Calculated	0.3606	1.0232	0.333	···	···	···

[a]Wyckoff positions for the $ThCr_2Si_2$-type structure [space group: $I4/mmm$ (No. 139)] are as follows: B at the 4e site [0, 0, z(boron)]; Co at the 4d site (1/2, 0, 1/4); and La at the 2a site (0, 0, 0).
[b]$R_{wp} = 4.93\%$, $R_I = 1.70\%$, and goodness of fit $S = 2.0$.

determined by electron microprobe analysis was $LaCo_2B_2$. The results of crystal structure refinements using synchrotron powder XRD are summarized in Table I, while the observed, calculated, and difference patterns are shown in Fig. 1(a). Structure relaxation calculations were performed using DFT. These revealed that the total magnetic moments were always zero even if U_{eff} of Co 3d was varied from 0 to 1.2 eV, corresponding to a non-spin-polarized ground state. The calculated lattice parameters reproduce experimental values with errors of less than 0.3%, and z(boron) on a 4e site agrees well with those obtained from Rietveld analyses, as summarized in Table I. Figure 1(a) also shows the determined crystal structure of $LaCo_2B_2$. In the structure, CoB and La layers are stacked alternately along the c axis. Each Co ion is coordinated by four B ions forming a fluorite-type layer, the length of each Co-B bond is 0.20 nm and the B-Co-B angles are 131° and 100°, indicating that the CoB layer is significantly compressed along the c axis. This structural feature is similar to that observed for the Co-P tetrahedral in LaCoPO with

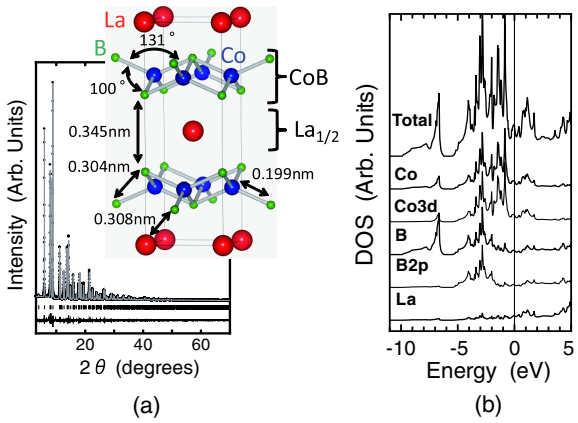

FIG. 1 (color online). (a) (Bottom) Observed synchrotron powder XRD pattern and results from Rietveld refinement for $LaCo_2B_2$. XRD data were collected by a Debye-Scherrer camera. The dots and lines indicate the observed and calculated patterns, respectively. The difference between the observed and calculated patterns is shown at the bottom. The vertical marks indicate the Bragg reflection positions for $LaCo_2B_2$. (Top) Crystal structure of $LaCo_2B_2$. (b) Calculated DOS of $LaCo_2B_2$, with the PDOS for La, Co, Co 3d, B, and B 2p.

P-Co-P angles of 123° and 103° [7]. In the fluorite-type layer, the Co ion occupies a 4d site with D_{2d} symmetry, resulting in the formation of a Co square lattice net. Note that the Co-Co distance in the net is 0.255 nm, which is very close to that in Co with a hexagonal close-packed arrangement (~ 0.250 nm) [19]. The B ion occupies a 4e site on a fourfold rotational axis, and resides at the apex of a square pyramid. Anionic B ions often prefer to condense in solids to form B-B bonds with a typical distance of 0.16–0.19 nm, as observed in FeB, and CaB_6 [20]. However, the obtained B-B distance of 0.34 nm between the Co-B layers in $LaCo_2B_2$ is far longer than that expected from the covalent radius of B (0.141 nm), indicating that interlayer B-B bonding is not present. Borides with a 122-type structure are quite rare except for Co borides [8], making this structure particularly unusual. It should also be noted that the La-B distance (0.308 nm) is significantly larger than their ionic or atomic radius (0.116 nm for La^{+3}) [21]. Isovalent doped compounds, $(La_{1-x}Y_x)Co_2B_2$, hole-doped compounds, $La(Co_{1-x}Fe_x)_2B_2$, and an electron-doped compound, $LaCo_2(B_{1-x}Si_x)_2$, were also successfully synthesized. The unit cell volume and lattice constants change monotonically with the ionic radii of the dopants (data not shown), indicating the formation of a solid solution up to $x = 0.20$, 0.30, and 0.10 for Y, Fe, and Si, respectively.

Figure 2(a) shows the resistivity-temperature (ρ-T) curve for $LaCo_2B_2$ and $(La_{1-x}Y_x)Co_2B_2$ ($x = 0$, 0.10) under an applied magnetic field of $H = 0$ Oe. The resistivity for $LaCo_2B_2$ ($x = 0$), which is a good metal, is $\sim 7 \times 10^{-5}$ Ω cm at 300 K, and it shows a small drop at 4 K. The Seebeck coefficient at 300 K is -7.4 μV/K, indicating that the electron carriers are responsible for conduction. No distinct peaks originating from magnetic transitions were observed down to 2 K in magnetic susceptibility measurements (data not shown), which indicates a Pauli PM state and is consistent with the calculated ground state. Substitution of Y into 10% of the La sites increases ρ, while the structure of the CoB conduction layer remains unchanged. The resistivity of the 10% Y-doped $LaCo_2B_2$ decreases almost linearly with T for $T > 130$ K. At $T < 20$ K, ρ shows a dependence of T^2, indicating a Fermi liquid state. As shown in the inset of

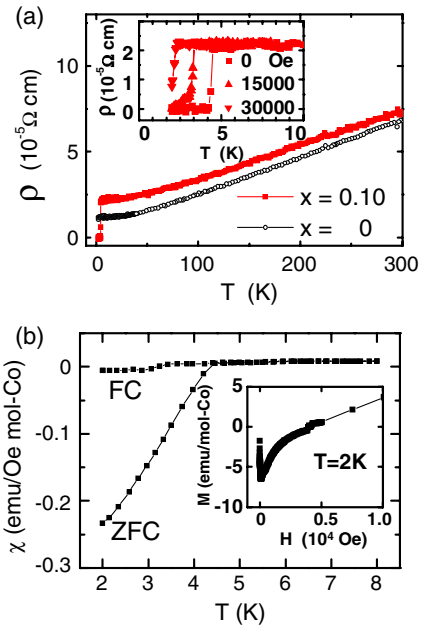

FIG. 2 (color online). (a) ρ-T plots for $(La_{1-x}Y_x)Co_2B_2$. The inset shows ρ-T curves for the sample with $x = 0.10$ as a function of magnetic field. (b) Temperature dependence of the magnetic susceptibility (χ) of $(La_{0.9}Y_{0.1})Co_2B_2$ under ZFC and FC conditions at 10 Oe. The inset shows the field dependence of magnetization at 2 K.

Fig. 2(a), a sharp drop in ρ was observed at $T = 4.4$ K, and disappeared at 4.1 K under zero magnetic field ($H = 0$ Oe). The zero-resistivity temperature decreases with increasing H, suggesting that 10% Y-doped $LaCo_2B_2$ undergoes a superconducting transition at 4.1 K. Figure 2(b) shows the temperature dependence of the magnetic susceptibility (χ) of 10% Y-doped $LaCo_2B_2$ measured in a zero-field cooling (ZFC) process and a field cooling (FC) process at 10 Oe. Between 4.2 and 300 K, χ was very small and nearly independent of temperature, implying Pauli PM. At 4.2 K, χ began to decrease, becoming negative and reaching -0.24 emu/mol-Co. This value corresponds to a shielding volume fraction of 15% (estimated from the χ value for perfect diamagnetism) at 2 K, which confirms that the bulk superconductivity transition occurs at 4.2 K. The M-H curve at 2 K presented in the inset of Fig. 2(b) shows a typical profile for a type-II superconductor with a lower superconducting critical magnetic field (H_{c1}) of ~90 Oe. It was confirmed that T_c did not depend on x.

Figure 3 shows ρ-T curves for $La(Co_{1-x}Fe_x)_2B_2$ ($x = 0$–0.30). Co doping of $x \geq 0.10$ induced superconductivity transitions at $T_c \sim 4$ K. Substitution of Fe into the Co site is expected to result in hole doping but the resistivity increased, which is explained by enhanced impurity scattering caused by direct doping of impurities into the CoB conduction layer. This is in sharp contrast to Co-doped $BaFe_2As_2$, where direct doping of Co in the FeAs conduction layer induces superconductivity but it is

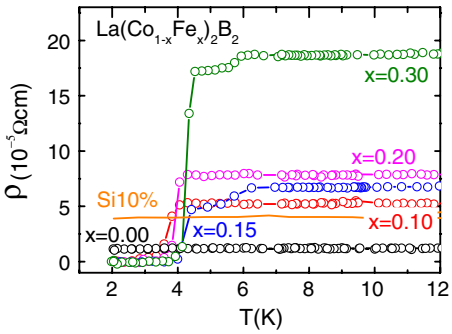

FIG. 3 (color online). ρ-T plots for $La(Co_{1-x}Fe_x)_2B_2$ ($x = 0$–0.3) and $LaCo_2(B_{1-x}Si_x)_2$ ($x = 0.10$).

expected to be electron doping [11]. On the other hand, substitution of Si into B sites raised the resistivity (e.g., ~4 times for $x = 0.1$) as the cases of other element doping, and did not induce a superconducting transition above 2 K.

The electronic nature of $LaCo_2B_2$ was investigated computationally as well as experimentally. Figure 1(b) shows partial density of states (PDOS) for $LaCo_2B_2$ calculated by DFT. The three following factors are evident: (1) La $4f$ and $5d$ levels are located >5 eV higher than the Fermi energy (E_F), (2) E_F is composed mainly of Co $3d$ and B $2p$ orbitals, and (3) PDOS of Co $3d$ and B $2p$ orbitals were similar to each other. (1) shows that the +3 charge state is the most stable for La in this compound because any introduced electrons would occupy the $4f$ and/or $5d$ levels that are located at much higher energy than E_F. A straightforward conclusion from (2) and (3) is that metallic conduction occurs in the CoB layer composed of highly covalent Co and B. Here, it is noted that B $2p$ levels are rather shallow compared with analogous 122-type pnictide compounds (As or P) in which As $4p$ and P $3p$ levels are much deeper than the transition metal $3d$ levels that primarily occupy E_F. The relatively shallow energy of anionic B $2p$ orbitals makes it difficult for it to adopt a closed shell state ($2p^6$) without the aid of a strongly positive cation. The shallow B $2p$ orbitals are not powerful enough to fully oxidize a Co ion. As a result, strong Co $3d$-B $2p$ covalent bonding forms a band with a width of 7.1 eV, removing the spin moment of the Co $3d$ electrons. This is in contrast to the ferromagnetic metal compounds LaCoXO (X = P or As), in which the formal charge of the Co ion can be regarded as +2 by assuming that of X to be -3 [7]. It is likely that the difference originates from the relatively deep energy of the As $4p$ level compared with that of B $2p$, and is similar to the relationship between LaFeAsO and LaFePO, where Fe $3d$ bands hybridized by broader P $3p$ and narrower As $4p$ levels [22] give rise to a PM state and AFM ordering, respectively.

Here we discuss the possible origin of the evolution of superconductivity caused by aliovalent (Fe) or isovalent (Y) substitution. The substitution of Fe into the Co site results in positive hole doping for optimization of carrier

concentration. Thus, this Fe doping is considered to raise positive hole concentrations to an optimal level for the appearance of superconductivity. We confirmed in the calculated DOS [Fig. 1(b)] that the E_F of the stoichiometric $LaCo_2B_2$ is located in the dip, similar to the case of $BaFe_2As_2$ [12], suggesting that the superconductivity in the Fe-doped $LaCo_2B_2$ would be similar to the K doping in $BaFe_2As_2$, although the parent compound has no magnetic ordering in $LaCo_2B_2$. On the other hand, the observed superconductivity in the Y-doped $LaCo_2B_2$ reminds us of the isovalent doping of P in $BaFe_2As_2$, which is considered to be driven by chemical pressure [10]. The other possible reason comes from the electron doping which occurs as a consequence of B-B dimer formation. This carrier doping idea was employed to control the valence state of the Co ion in Co pnictides with the 122-type structure [23]. Although we have not examined the precise modification of the B-B distance in the doped $LaCo_2B_2$ upon doping, it is unlikely that electron doping induces a superconducting transition, on the basis of experimental results [no T_c was observed on $LaCo_2(B_{1-x}Si_x)_2$].

The electrical and magnetic properties of $LaCo_2X_2$ (X = P, Si, or B) at low temperature are changed significantly by varying X from P to B: the materials are ferromagnetic with T_{Curie} = 103 K for P [24], PM metallic conductor for Si [25], and superconductor for B. Anionic substitution of the parent $LaCo_2B_2$ with P or Si corresponds to electron doping. A variety of derivatives can be synthesized by doping La, Co, or X sites, which allows for the systematic study of superconductivity.

In summary, we found that $LaCo_2B_2$ composed of alternate stacked layers of La and CoB exhibits bulk superconductivity with a T_c of ~4 K upon cationic substitution. The appearance of superconductivity by isovalent or aliovalent substitution suggests that the highly covalent CoB layer is responsible for superconductivity by the introduction of a small perturbation, such as chemical pressure caused by the formation of a solid solution.

This work was supported by the Funding Program for World-Leading Innovative R&D on Science and Technology (FIRST), Japan. We thank Dr. J. Kim (JASRI), Dr. S. W. Kim, and Dr. H. Hiramatsu (Tokyo Tech) for XRD measurements.

*Corresponding author.
hosono@lucid.msl.titech.ac.jp

[1] Y. Kamihara *et al.*, J. Am. Chem. Soc. **130**, 3296 (2008).
[2] Z. Ren *et al.*, Chin. Phys. Lett. **25**, 2215 (2008).
[3] R. J. Cava *et al.*, Nature (London) **367**, 252 (1994).
[4] K-H. Muller and V. N. Narozhnyi, Rep. Prog. Phys. **64**, 943 (2001).
[5] K. Tsutsumi *et al.*, J. Phys. Soc. Jpn. **64**, 2237 (1995).
[6] K. Takada *et al.*, Nature (London) **422**, 53 (2003). Superconductivity occurs in Na_xCoO_2 with 2D CoO_2 layer by the chemical oxidation process.
[7] H. Yanagi *et al.*, Phys. Rev. B **77**, 224431 (2008).
[8] K. Niihara, T. Shishido, and S. Yajima, Bull. Chem. Soc. Jpn. **46**, 1137 (1973).
[9] M. Rotter, M. Tegel, and D. Johrendt, Phys. Rev. Lett. **101**, 107006 (2008).
[10] S. Jiang *et al.*, J. Phys. Condens. Matter **21**, 382203 (2009).
[11] D. Mandrus *et al.*, Chem. Mater. **22**, 715 (2010).
[12] D. J. Singh, Phys. Rev. B **78**, 094511 (2008).
[13] F. Izumi and K. Momma, Solid State Phenom. **130**, 15 (2007).
[14] G. Kresse and J. Furthmuller, Phys. Rev. B **54**, 11 169 (1996).
[15] P. E. Blochl, Phys. Rev. B **50**, 17 953 (1994).
[16] G. Kresse and D. Joubert, Phys. Rev. B **59**, 1758 (1999).
[17] K. Ueda, H. Hosono, and N. Hamada, J. Phys. Condens. Matter **16**, 5179 (2004).
[18] K. Kuroki *et al.*, Phys. Rev. Lett. **101**, 087004 (2008).
[19] L. J. E. Hofer and W. C. Peebles, J. Am. Chem. Soc. **69**, 893 (1947).
[20] A. F. Wells, *Structural Inorganic Chemistry* (Clarendon Press, Oxford, 1986), 5th ed.
[21] R. D. Shannon, Acta Crystallogr. Sect. A **32**, 751 (1976).
[22] V. Vildosola *et al.*, Phys. Rev. B **78**, 064518 (2008).
[23] S. Jia and R. J. Cava, Phys. Rev. B **82**, 180410(R) (2010).
[24] M. Reehuis *et al.*, J. Magn. Magn. Mater. **138**, 85 (1994).
[25] H. Mizoguchi *et al.* (unpublished).